

Microwave rf SQUID integrated into a planar YBa₂Cu₃O₇ resonator

Y. Zhang, M. Mück, M. Bode, K. Herrmann, J. Schubert, W. Zander,
A. I. Braginski, and C. Heiden

Institute of Thin Film and Ion Technology, Research Center Jülich (KFA), D-5170 Jülich, Germany

(Received 18 December 1991; accepted for publication 27 February 1992)

We fabricated and characterized microwave rf SQUIDs integrated into a planar, S-shaped $\lambda/2$ microstrip resonator. This 3 GHz resonator was fabricated from a pulsed-laser-deposited YBa₂Cu₃O₇ epitaxial film. The SQUID structures incorporated double step-edge junctions and had a loop inductance of 120 pH. Such unoptimized SQUIDs operated between 4.2 and 85 K with $dV/d\Phi = 18\text{--}20 \mu\text{V}/\Phi_0$ at 77 K. At that temperature, the energy resolution of $(8 \pm 2) \times 10^{-29}$ J/Hz above 0.1 Hz (in the best samples) was limited by the white noise, $S_{\Phi}^{1/2} = (7 \pm 1) \times 10^{-5} \Phi_0/\text{Hz}^{1/2}$. Optimization may increase $dV/d\Phi$ and improve the energy resolution by up to an order of magnitude.

We have been investigating microwave rf SQUIDs integrated into a microstrip $\lambda/2$ resonator fabricated from epitaxial YBa₂Cu₃O₇ (YBCO) thin films. Our main motivation has been to exploit the possibilities of flux noise reduction in YBCO rf SQUIDs capable of operating at high temperatures, up to 77 K. It is well known that the rf SQUID signal power is proportional to the tank frequency, ω_T . Hence, for uncorrelated noise, the energy resolution improves with increasing ω_T , up to the critical frequency, $\omega_c = R_n/L_s$, where R_n is the junction resistance and L_s the SQUID loop inductivity. The frequency limit is even higher than ω_c for the hysteretic mode of SQUID operation.² Daly *et al.*³ reported recently on the first microwave YBCO SQUID which was coupled to a 10 GHz TE₀₁₁ cylindrical cavity and operated at 55 K. However, no noise and energy resolution data were presented. We have recently shown⁴ that at $\omega_T = 150$ Mz both the $1/f$ and the white noise in YBCO rf SQUIDs with step-edge junctions were significantly lower than at $\omega_T = 20$ MHz. To further increase ω_T by over an order of magnitude, we implemented in YBCO the concept of a planar, integrated microwave SQUID first demonstrated in low-temperature Nb technology.⁵ We also used the 3 GHz flux-locked SQUID read-out electronics developed for its characterization.⁶ Preliminary results, obtained with an arbitrarily chosen $L_s = 120$ pH, are presented below.

The layout of the S-shaped microstrip resonator with the SQUID loop in its central segment is shown in Fig. 1. According to simulation,⁷ the geometrical length of a $\lambda/2$ resonator on a (100) LaAlO₃ substrate ($\epsilon = 25$) should be 13.5 mm at 3.0 GHz. A length of 16 mm was deduced from measurement of test resonators. We used the S-shape to minimize the largest linear dimension of the YBCO resonator. It could thus be patterned in the central, most homogeneous area of a standard 10×10 mm² YBCO chip. To insure an adequate impedance matching, the $100 \times 100 \mu\text{m}^2$ SQUID hole (labeled "1" in Fig. 1) with the weak link (labeled "2") were placed at the voltage node in the center of the resonator. The weak link, bridging the slit in the resonator body, consisted of a series connection of two step-edge junctions. The junctions, $2 \mu\text{m}$ apart, were formed by positioning a $2\text{-}\mu\text{m}$ wide and $10\text{-}\mu\text{m}$ -long YBCO bridge (labeled "3") across two $0.25 \mu\text{m}$ high steps in the

substrate introduced by a $2\text{-}\mu\text{m}$ -wide local pit (labeled "4"). We have shown earlier⁸ that the use of only one step, which extends across the whole substrate, leads to a high $1/f$ noise contribution from the wide branch of the rf SQUID washer bridging the step. Two narrow step-edge junctions contribute to rf and dc SQUIDs a relatively low $1/f$ flux noise.^{4,9} The rf SQUID response is generally determined by the lower I_c junction.¹⁰ The microstrip configuration was formed by the 0.5-mm -thick LaAlO₃ substrate and a copper ground plane. The resonator was capacitively coupled to a 50Ω coaxial cable leading to the room-temperature electronics. This coupling was adjustable at room temperature but not during the measurement. For each sample, the coupling has been set to obtain the highest

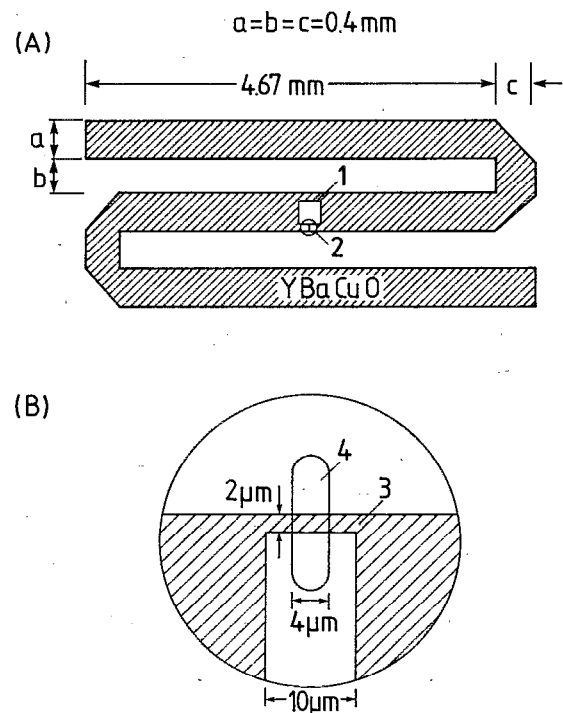


FIG. 1. (a) Layout of the microwave SQUID resonator; 1—the $100 \times 100 \mu\text{m}^2$ SQUID hole, 2—area encompassing the $10 \mu\text{m}$ wide slit bridged by the weak link, (b) magnified area 2 of (a); 3—YBCO bridge, 4—local pit in the substrate.

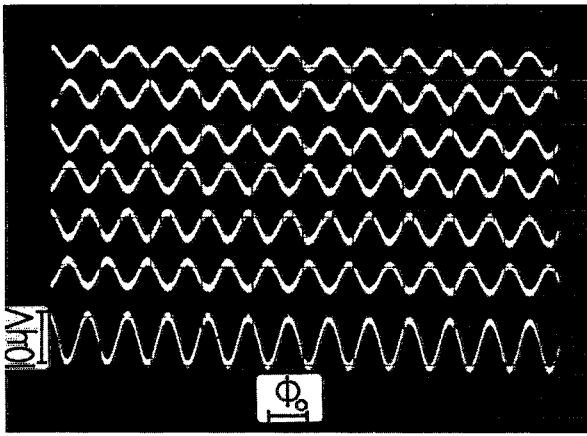


FIG. 2. SQUID signal at 77 K at different microwave power levels corresponding to the first seven steps in the rf I - V characteristics; $\beta_L > 1$. The vertical scale is 10 $\mu\text{V}/\text{div}$, i.e., the signal amplitude on the first step is $V_{pp} = 10 \mu\text{V}$.

possible value of the transfer function of the SQUID, $\delta V/\delta \Phi$.

The microwave SQUID structures were patterned by optical photolithography. The patterns were transferred by ion-beam etching onto 200–250 nm thick epitaxial YBCO films deposited by pulsed laser deposition. The patterned local pit in the substrate (“4” in Fig. 1) was ion-beam etched through a metal mask. Details of the fabrication process were nearly identical with those described earlier.^{4,8}

We characterized three SQUID samples with different values of the SQUID parameter $\beta_L = 2\pi I_c L_s / \Phi_0$, where I_c is the critical current of the junction. The $\beta_L < 1$, and > 1 was inferred from the rf I - V characteristics measured at 77 K using the 150 MHz electronics.⁴ The resonators were characterized using the reflection method by means of a HP 8510 network analyzer and had nearly identical properties. The center frequency of the structure shown in Fig. 1 was about 3.25 GHz. It changed by only 56 MHz over the temperature range from 4.2 to 77 K, thus indicating a satisfactory homogeneity of the resonator. Resonators without the integrated SQUID loop had a high Q ranging from over 10 000 at 4.2 K to approximately 3000 at 77 K. However, resonators with SQUID showed a loaded Q of only 300–400 at 4.2 K to over 200 at 77 K. Simulation gave a $Q = 150$ for an arbitrarily chosen coupling via an 80 μm gap in the microstrip and LaAlO_3 $\tan \delta = 2 \times 10^{-4}$. The measuring rf power of the analyzer was very high, about 1 mW, compared to the SQUID dissipation, of the order of 10 pW, at the first rf step. It is not clear whether during the Q measurement the SQUID was operating, and thus loading the resonator. Losses in the weak link should reduce Q significantly. Also, the coupling between the resonator and transmission line, set for optimum $\delta V/\delta \Phi$, was relatively strong thus reducing the loaded Q .

Near 3.25 GHz, all three SQUIDs operated between 4.2 and 85 K in the flux-locked mode. The signal voltage, shown in Fig. 2 for the first seven steps in the rf I - V characteristics, was nearly temperature independent for two

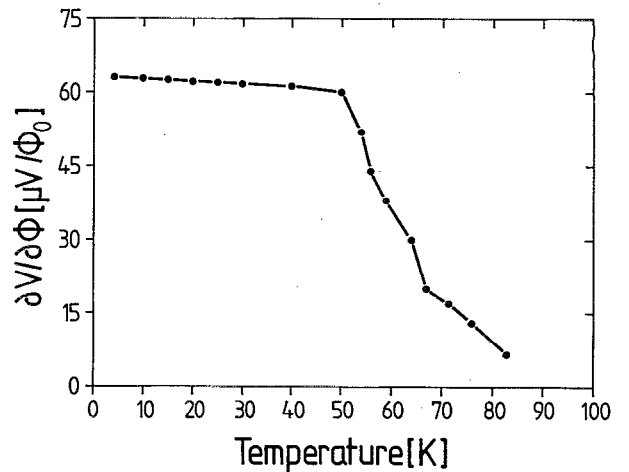


FIG. 3. Temperature dependence of $\delta V/\delta \Phi$; $\beta_L < 1$ at 77 K.

SQUIDs having $\beta_L > 1$. At low temperatures, these two SQUIDs exhibited changes in the signal shape, typical of a hysteretic I - V characteristic of the weak link. The signal amplitude of the SQUID having $\beta_L < 1$ at 77 K increased when the temperature decreased down to about 50 K and remained approximately constant at still lower temperatures where, presumably, $\beta_L > 1$. This temperature dependence is shown in Fig. 3. At 55 K, where $\beta_L = 1$, $\delta V/\delta \Phi = 60 \mu\text{V}/\Phi_0$ and the white flux noise above 50 Hz was $S_\Phi^{1/2} = 3 \times 10^{-5} \Phi_0/\text{Hz}^{1/2}$. The corresponding SQUID energy resolution was $\epsilon = 1.6 \times 10^{-29} \text{ J/Hz}$.

A more detailed characterization of the SQUIDs was performed at 77 K. At that temperature, the best performance was obtained for $\beta_L > 1$. The value of the transfer function was $\delta V/\delta \Phi = 18\text{--}20 \mu\text{V}/\Phi_0$. The white flux noise was $S_\Phi^{1/2} = (7 \pm 1) \times 10^{-5} \Phi_0/\text{Hz}^{1/2}$ with a crossover to $1/f$ below 0.1 Hz in one SQUID and below 1 Hz in another. The noise characteristics of the best sample are shown in Fig. 4. The corresponding energy resolution above the crossover frequency is $\epsilon = (8 \pm 2) \times 10^{-29} \text{ J/Hz}$. All the noise measurements were performed in a mumetal-shielded, low self-noise fiberglass dewar.

To our knowledge, the $1/f$ flux noise level shown above is the lowest thus far reported for a high-temperature rf SQUID. However, at 77 K, the white noise level is only marginally lower than that at 150 MHz [$S_\Phi^{1/2} = (8\text{--}15) \times 10^{-5} \Phi_0/\text{Hz}^{1/2}$] determined in washer rf SQUIDs.⁴ At 3 GHz, scaling with ω_T should lead to a 4.5 lower $S_\Phi^{1/2}$ level than at 150 MHz. Since $S_\Phi^{1/2} = S_v^{1/2}/\delta V/\delta \Phi$, the much higher than expected flux noise at 3 GHz is the consequence of the transfer function value being an order of magnitude lower than that determined, using the same electronics, in nearly identical niobium SQUID structures with junctions of similar R_n .

We examined possible reasons for the reduced $\delta V/\delta \Phi$. The upper frequency limit to useful SQUID response has not been exceeded, as shown by the niobium SQUID data. Indeed, with the typical R_n value of $5 \pm 1 \Omega$ for two YBCO step-edge junctions in series, the critical frequency $\omega_c/2\pi = 6.6 \text{ GHz}$ clearly exceeds $\omega_T/2\pi$. However, one likely reason for a depressed $\delta V/\delta \Phi$ at 77 K could be the effec-

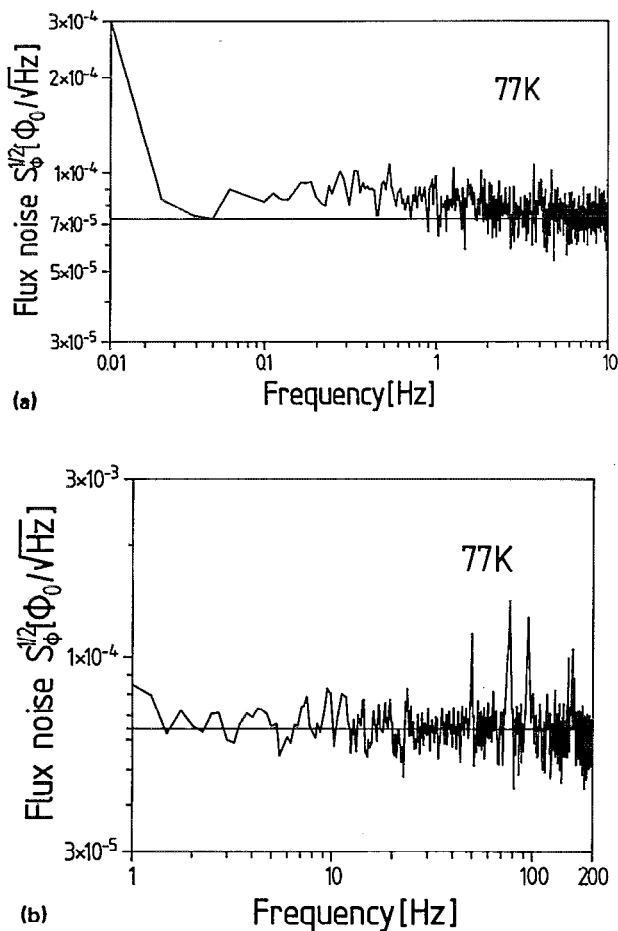


FIG. 4. Noise spectra of the best sample at 77 K: (a) between 0.01 and 10 Hz, marker at $7.3 \times 10^{-5} \Phi_0/\text{Hz}^{1/2}$; (b) between 1 and 200 Hz, marker at $6.4 \times 10^{-5} \Phi_0/\text{Hz}^{1/2}$. Measurements performed at different times.

tive shunt capacitance of the step-edge junction, C_j , which includes the stray capacitance of the SQUID structure. In SQUIDs with β_L (77 K) $\gg 1$ the junctions are hysteretic at low temperature and the McCumber parameter $\beta_c = (2e/h)I_c C_j R_n^2 > 1$. A simple numerical estimate for $\beta_c = 1$ –10 shows that at 3 GHz the capacitive shunt admittance can be comparable to R_n . The improvement in $\delta V/\delta \Phi$ will thus be obtained by reducing the effective C_j .

Another reason for the $\delta V/\delta \Phi$ depression in our YBCO SQUIDs is that the condition $k^2 Q = 1$ is not ful-

filled. The estimate of the magnetic coupling coefficient in the integrated SQUID-resonator structure¹¹ is $k^2 = 10^{-3}$. With a loaded $Q = 200$ at 77 K, $k^2 Q = 0.2$. In contrast, the Nb-SQUID has a loaded Q is 600 to 1000, depending on the coupling to the transmission line, so that $k^2 Q$ approaches one. In the YBCO SQUIDs, one should thus increase the SQUID-resonator coupling through geometrical modifications of the integrated structure. Alternatively, one can attempt to increase the loaded Q sufficiently. Experimental data for a lower tank frequency¹² and our results obtained at 55 K indicate that the low $k^2 Q$ alone can be responsible for a depression of $\delta V/\delta \Phi$ by a factor of 2–3 but not by an order of magnitude.

Both optimization directions appear promising. Above the crossover to $1/f$ noise, we expect the optimized YBCO SQUID to have an energy resolution at 77 K much better than $\epsilon = 1 \times 10^{-29}$ J/Hz. The calculated intrinsic SQUID noise¹³ at that temperature leads to $\epsilon = 5 \times 10^{-31}$ J/Hz.

We express our thanks to Th. Pecks (University of Duisburg) for the simulation of the resonator structure and acknowledge a partial support of the BMFT Consortium "First Applications of HTS in Micro- and Cryoelectronics."

¹J. Kurkijärvi, Phys. Rev. B 6, 832 (1972).

²R. A. Buhrman and L. D. Jackel, IEEE Trans. Magn. 13, 879 (1977).

³K. P. Daly, J. Burch, S. Coons, and R. Hu, IEEE Trans. Magn. 27, 3066 (1991).

⁴Y. Zhang, H.-M. Mück, K. Herrmann, J. Schubert, W. Zander, A. I. Braginski, and C. Heiden, Appl. Phys. Lett. 60, 645 (1992).

⁵M. Mück and C. Heiden, *Extended Abstracts of the Second International Superconductive Electronics Conference (ISEC '89)* (Jpn. Soc. of Appl. Phys., Tokyo, 1989), p. 199; M. Mück, D. Diehl, and C. Heiden, Cryogenics 30, 1149 (1990).

⁶M. Mück, Rev. Sci. Instrum. (to be published).

⁷Simulation performed by Th. Pecks (University of Duisburg) using his "Spectral Domain" software.

⁸K. Herrmann, Y. Zhang, H.-M. Mück, J. Schubert, W. Zander, and A. I. Braginski, Supercond. Sci. Technol. 4, 583 (1991).

⁹G. Friedl, M. Vildic, M. Römhild, B. Roas, D. Uhl, F. Bömmel, G. M. Dalmaans, B. Hillenbrand, and H. E. Hoenig, in Proc. 4th Int. Symposium on Superconductivity (ISS'91), Springer-Verlag Tokyo, Inc., Tokyo 1992 (to be published).

¹⁰Y. Zhang and C. Heiden, in *Advances in Cryogenic Engineering*, edited by A. F. Clark and R. P. Reed (Plenum, New York, 1988), Vol. 34, pp. 781–787.

¹¹M. Mück and C. Heiden, Appl. Phys. A (to be published).

¹²D. Pascal and M. Sauzade, J. Appl. Phys. 45, 3085 (1974).

¹³J. Kurkijärvi, J. Appl. Phys. 44, 3729 (1973).